Aluminum Inhibits the H^+-ATPase Activity by Permanently Altering the Plasma Membrane Surface Potentials in Squash Roots[1]

Sung Ju Ahn, Mayandi Sivaguru[2], Hiroki Osawa, Gap Chae Chung, and Hideaki Matsumoto*

Research Institute for Bioresources, Okayama University, Chuo 2–20–1, Kurashiki 710–0046, Japan (S.J.A., M.S., H.O., H.M.); Department of Horticulture, Biotechnology Research Institute, College of Agriculture, Chonnam National University, Kwangju 500–757, Korea (S.J.A, G.C.C.); and Bio-Oriented Technology Research Advancement Institution, Omiya 331–8637, Japan (H.O.)

Although aluminum (AL) toxicity has been widely studied in monocotyledonous crop plants, the mechanism of Al impact on economically important dicotyledonous plants is poorly understood. Here, we report the spatial pattern of Al-induced root growth inhibition, which is closely associated with inhibition of H^+-ATPase activity coupled with decreased surface negativity of plasma membrane (PM) vesicles isolated from apical 5-mm root segments of squash (*Cucurbita pepo* L. cv Tetsukabuto) plants. High-sensitivity growth measurements indicated that the central elongation zone, located 2 to 4 mm from the tip, was preferentially inhibited where high Al accumulation was found. The highest positive shifts (depolarization) in zeta potential of the isolated PM vesicles from 0- to 5-mm regions of Al-treated roots were corresponded to pronounced inhibition of H^+-ATPase activity. The depolarization of PM vesicles isolated from Al-treated roots in response to added Al in vitro was less than that of control roots, suggesting, particularly in the first 5-mm root apex, a tight Al binding to PM target sites or irreversible alteration of PM properties upon Al treatment to intact plants. In line with these data, immunolocalization of H^+-ATPase revealed decreases in tissue-specific H^+-ATPase in the epidermal and cortex cells (2–3 mm from tip) following Al treatments. Our report provides the first circumstantial evidence for a zone-specific depolarization of PM surface potential coupled with inhibition of H^+-ATPase activity. These effects may indicate a direct Al interaction with H^+-ATPase from the cytoplasmic side of the PM.

Although plant Al toxicity has been recognized for at least a century, the specific mechanism by which Al inhibits root elongation is yet to be determined (Horst, 1995; Kochian, 1995; Taylor, 1995; for recent reviews, see Matsumoto, 2000). However, recent advances in this field have led to a general understanding that the root apex plays a central role in the mechanism of Al toxicity, as it is the target site for Al-induced root growth inhibition (Ryan et al., 1993; Kochian, 1995; Sivaguru and Horst, 1998). Much of the previous research on Al toxicity has focused on monocotyledonous crop plants such as wheat and maize, and a detailed analysis of potential mechanisms of Al-induced inhibition of root growth in dicotyledonous plants has not been conducted previously.

While the apoplastic and symplastic target sites of Al in plant cells are under debate (Horst, 1995; Kochian, 1995; Rengel, 1996), several studies have focused on the plasma membrane (PM) as having a key function. PM properties such as surface negativity or zeta potential have been reported to be altered by Al and may be important as barriers to the passive movement of Al into root cells (Miyasaka et al., 1989; Wagatsuma and Akiba, 1989; Kinraide 1994; Yermiyahu et al., 1997; Kinraide et al., 1998). The differing PM negative electrical charges among plants are expected to differentially attract the positively charged Al ions (Kinraide et al., 1992) and may alter phospholipid profile thereby affecting lipid-mediated signaling (Jones and Kochian, 1997). Such alterations to membrane electrical properties may destabilize the PM. Yermiyahu et al. (1997) elucidated the mechanisms underlying differences in surface-charge density using PM vesicles isolated from whole-root, root tips, and tip-less roots of wheat (cv Scout 66 and cv Atlas 66). The surface charge of the PM depends on both biotic and abiotic factors such as the external pH. Al has been shown to inhibit calmodulin-stimulated, membrane-bound ATPase

[1] This work was supported by the Program for the Promotion of Basic Research Activities in Innovative Biosciences; by the Ministry of Agriculture, Forests and Fisheries, Japan (to H.M.); by the Ministry of Education, Science, Sports and Culture of Japan (Grant-in-Aid for General Scientific Research [A] to H.M.); by the Japan (to H.M.)-Korea (to G.C.C.) Joint Research Project supported by the Japan Society for the Promotion Science and Korea Science and Engineering Foundation (grant no. 986–0500–001–2); by the Basic Scientific Cooperation Program "Research for the Future" Program; and by the Japan Society for the Promotion Science, Ohara Foundation for Agricultural Sciences (postdoctoral fellowship to M.S.).

[2] Present address: Division of Biological Sciences, 109 Tucker Hall, University of Missouri, Columbia, MO 65211–7400.

* Corresponding author; e-mail hmatsumo@rib.okayama-u.ac.jp; fax 81–86–434–1249.

activity, which regulates the H^+ fluxes across the PM and the maintenance of trans-membrane potential (Siegel and Haug, 1983; Matsumoto et al., 1992). A decrease in PM surface potential is correlated with the decline in H^+-ATPase activity in isolated PM vesicles of tomato roots under salt stress (Suhayda et al., 1990). In line with this, Gimmler et al. (1991) proposed a close relationship between zeta potential and PM H^+-ATPase activity and emphasized the importance of zeta potential in cation toxicity. Kinraide (1994) and coworkers (1998) recently (see above) modified the Gouy-Chapman-Stern model and developed a computer program to demonstrate the near-equal-binding constants of H^+ and Al to the negatively charged surface sites of the plant cell membranes. The computed Al activities on the surface of the PM were correlated with the surface charge, which is in turn correlated with root growth. It has been generally accepted that differences in the resting surface potential among plant species may play an important role in determining the uptake of cations, including Al, and thus contribute to genotypic differences in the Al sensitivity.

H^+-ATPase is a "master enzyme" located preferentially at the epidermal and cortical cell layers of roots (Jahn et al., 1998) and plays a central role in the functional association of PM surface charge with H^+ efflux/influx and thus the regulation of cytoplasmic pH in response to a variety of environmental stimuli. Furthermore, as H^+-ATPase is an abundant PM protein accounting for approximately 5% of root PM proteins (Serrano, 1985; Sussman, 1994), the modulation in their activity is a crucial factor for the survival of plants when they are under a variety of environmental stresses, such as low root temperature (Ahn at al., 1999), salt stress (Suhayda et al., 1990), and low pH (Yan et al., 1998). In addition, Young et al. (1998) analyzed Arabidopsis transgenic plants expressing one of the PM H^+-ATPase (AHA3) with an altered C terminus and demonstrated that they were more resistant to acid medium than the wild-type counterparts.

Since the proposal of Vose and Randall (1962) that the negative surface-charge densities may play an important role in Al tolerance mechanisms, intensive research has been triggered in this area by studying cell surface electrical properties of PM in relation to H^+ efflux and influx upon Al treatment. A few correlations have been obtained between surface potential and Al tolerance in plants such as wheat (Kinraide, 1988, 1994; Kinraide et al., 1992, 1998; Yermiyahu et al., 1997), maize, and barley (*Hordeum vulgaris* L. cv Kikaihadaka; Wagatsuma and Akiba 1989). However, there has not been any study to our knowledge integrating both the electrical properties of PM and alteration of H^+-ATPase activity along the various zones of root apex in response to Al toxicity. Therefore, using a poorly understood dicotyledonous squash (*Cucurbita pepo* L.) plant, we demonstrate the spatial differences in Al-induced growth inhibition and Al accumulation, both of which have an inherent relationship with the H^+-ATPase activity and surface potential of PM vesicles isolated from specific 5-mm root segments.

RESULTS

Spatial Pattern of Root Growth Inhibition by Al

There was a significant inhibition in root growth at both 3 and 6 h after a 50 μM Al treatment (data not shown). All subsequent experiments were performed with roots grown in the presence or absence of 50 μM Al. In the case of segmental elongation, control roots showed the disappearance of 2- and 4-mm marks after 3 and 6 h (Fig. 1, A′ and A″), respectively. But the 2-mm mark faded after 3 and 6 h in the roots treated with Al (Fig. 1, B′ and B″). The marks (white

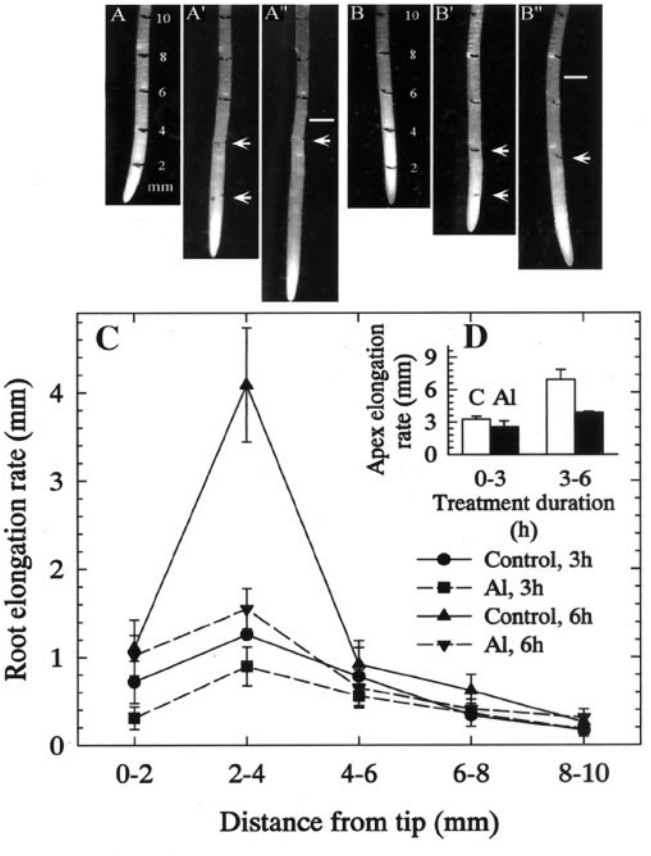

Figure 1. Effect of Al (50 μM) on the segmental elongation rate (sets A–A″, B–B″, C, and D) of squash roots. Sets A, A′, and A″ were for control roots at 0, 3, and 6 h, respectively, marked with India ink at 2-mm intervals at 0 h. Sets B, B′, and B″ represent roots treated with 50 μM Al for the same time points. Arrows denote the 2- and 4-mm positions after 3 h (A′ and B′) and subsequent alteration to their position after 6 h (A″ and B″). Bars in A″ and B″ denote a distance of from the root tip 10 mm after 6 h. C, Elongation rate of 2-mm root regions in control and Al treatments after 3 and 6 h. D, Increment in total elongation of the apex (10 mm) during 0 to 3 and 3 to 6 h. Values in C and D are mean ± SE of six replicates and representative of three independent experiments.

bars) made 10 mm from the apex of roots extended approximately 5- (control) and 3-mm (Al) distances from their initial position at 0 h, indicating a clear inhibition of growth by Al (Fig. 1, A″ and B″). From the Figure 1C, it was apparent that the 2- to 4-mm region had the highest elongation rate in both control and Al-treated roots. The latter exhibited dramatic inhibition in this region after 3 (50%) and 6 h (75%), whereas all other regions did not significantly contribute to root growth. In the elongation rate of total apex (10 mm) (Fig. 1D), the above details on the inhibitory effect of Al at 2 to 4 mm could not be observed.

We quantified Al contents in 2-mm root segments as well as from the whole-root apex (10 mm). In agreement with growth pattern after 3-h Al treatments, higher Al accumulations were found in the 0- to 2- and 2- to 4-mm segments but declined sharply in the 4- to 6-mm segment. Although a similar trend was observed after 6 h, there was a 35% increase in Al accumulation in all other segments including the 0- to 2-mm segment (Fig. 2A). As described above for the differences between the whole root and segmental elongation rates, the extent of Al accumulation was also masked while measuring the total root Al contents compared with segmental Al contents (Fig. 2B).

Impact of Al on Zeta Potential and the H+-ATPase Activity of PM Vesicles

Substantial increase in H+-ATPase activity using vesicles collected from 10-mm root apices was observed with the addition of Brij 58, indicating that approximately 85% of the vesicles were sealed, right-side-out, and of high-purity. The purity of PM vesicles was validated in the presence and absence of

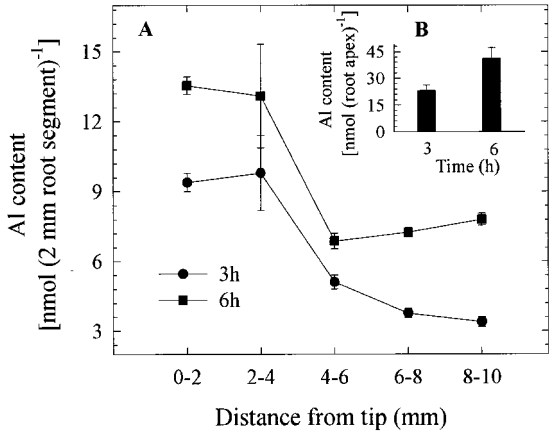

Figure 2. Effect of Al (50 μM) on the Al accumulation at 2-mm specific segments (A) and in the total root (10-mm) apex (B) of squash plants after 3- and 6-h Al treatments. Al was not detected in control root apices. The Al contents were determined either in three replicates, each comprising three 10-mm root apices for the total apex or in five replicates each comprising five 2-mm segments of the same distance from the tip (DFT) position. Values are mean ± SE and representative of at least two independent experiments.

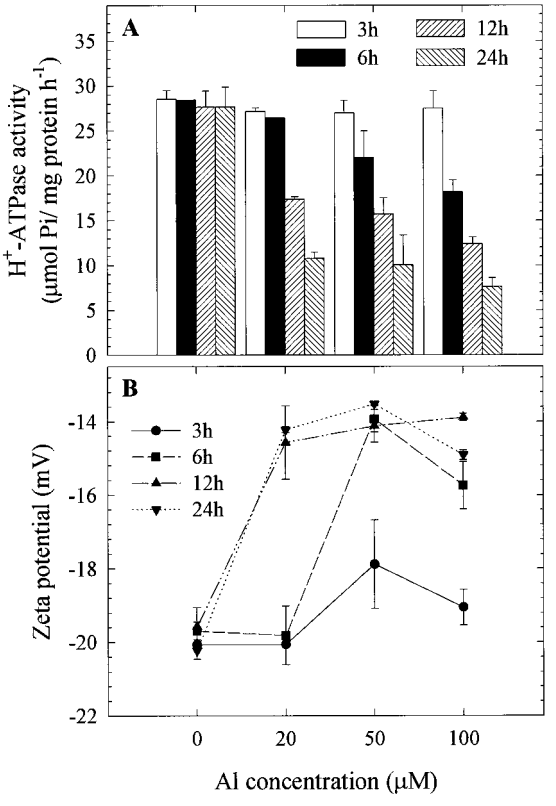

Figure 3. Effect of a range of Al concentrations (0, 20, 50, and 100 μM) and treatment durations (3, 6, 12, and 24 h) on the H+-ATPase activity (A) and zeta potential (B) of PM vesicles isolated from whole-root fractions of squash. The plants were grown in HS (1/5) adjusted to pH 4.5 for 5 d from germination. Al treatments were performed in the same solution without P and the plants were cultured in −P solution for at least 12 h prior to treatments. Values are mean ± SE of three replicates and representative of two independent experiments. Al was absent in the electrophoresis medium.

various inhibitors. Vanadate, which is a specific inhibitor of PM ATPase activity, inhibited by approximately 90% of the activity, whereas nitrate and azide caused less than 10% inhibition (data not shown).

To investigate the Al-impact on zeta potential and H+-ATPase activity of PM vesicles, we exposed the squash plants to a range of Al concentrations (0, 20, 50, and 100 μM) for different durations (3, 6, 12, and 24 h). We found a clear increase in zeta potential of whole-root PM vesicles associated closely with the decrease in H+-ATPase activity under increasing Al concentration and treatment duration (Fig. 3, A and B). These results indicated that a close association between zeta potential and H+-ATPase activity does exist under Al toxicity. However, the intricacies of this relationship were not clear, and whether they are directly linked and/or dependent on each other has yet to be investigated.

In addition, the in vitro effect of Al on zeta potential was analyzed using whole-root PM vesicles of control plants. The PM vesicles were subjected to various concentrations of Al in vitro. The surface

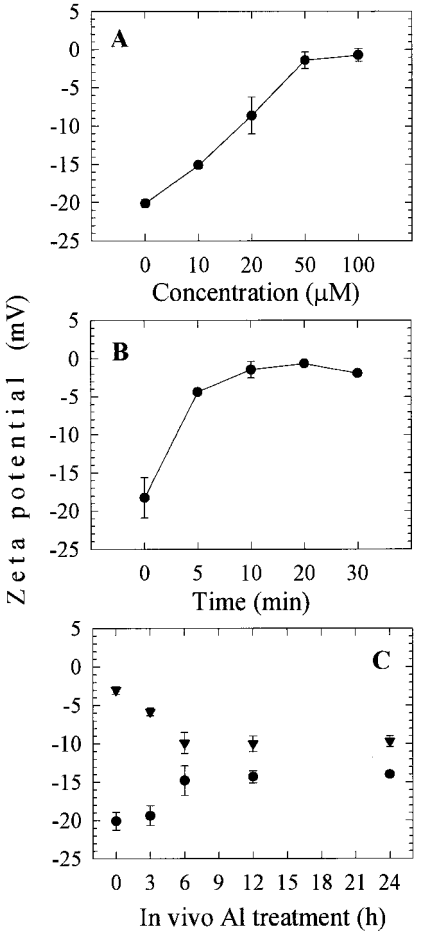

Figure 4. Effect of Al (50 μM) in vitro on the zeta potential of PM vesicles isolated from whole-root fractions of squash. The plants were grown in HS (1/5) adjusted to pH 4.5 for 5 d from germination and cultured in −P solution for at least 12 h prior to isolation without Al. The control PM vesicles were subjected to a range of Al concentrations (A) and treatment duration (B) in vitro. In a parallel experiment, the PM vesicles isolated after 0, 3, 6, 12, and 24 h (C) 50 μM Al treatments in vivo (●) then they were subjected again to 50 μM Al in vitro for 10 min (▼). Values are mean ± SE of at least two independent experiments.

potential of control PM vesicles was dramatically depolarized at 50 μM Al after 10 min (Fig. 4, A and B). It should be noted here that the electrophoresis medium buffer was set at pH 7.4 to maintain the functional integrity of the PM vesicles during measurements. In this medium under such pH environment one can obviously predict most of the added Al will not exist in the form of Al^{3+}. Hence, we cannot exclude the fact that the observed PM depolarization might be caused due to other factors rather than Al^{3+} or even Al in the form of complexes with other ligands. Since we were aware of the response of control PM vesicles and the Al impact in in vivo, we continued the surface potential measurements with PM vesicles isolated from whole roots subjected to 50 μM Al for 0, 3, 6, 12, and 24 h. After the treatments of whole roots the PM vesicles were isolated and subjected again to Al in vitro. It is interesting that the zeta potentials of PM vesicles prepared from both control and Al-treated roots after 3 h exposure increased markedly from −20 mV to −1 mV, but PM vesicles prepared from the Al treated for 6, 12, and 24 h exhibited less depolarization (Fig. 4C).

We also analyzed the segmental differences in both zeta potential and H^+-ATPase activity as influenced by Al in vivo. Since the 2- to 4-mm region was the sensitive target site for 50 μM Al, as described earlier (Fig. 1), we used 0- to 5-mm individual root segments for this purpose. The segmental analysis revealed that the zeta potential was more negative (−22.6 mV) in the 0- to 5-mm segments compared with other segments of the control roots. A significant increase (from −22.6 to −15 mV) in zeta potential was observed only in PM vesicles from 0- to 5-mm segments after 3- and 6-h Al treatments compared with the other segments analyzed (Fig. 5B). Congruent with zeta potential, H^+-ATPase activity of PM vesicles prepared from 0- to 5-mm roots was approximately

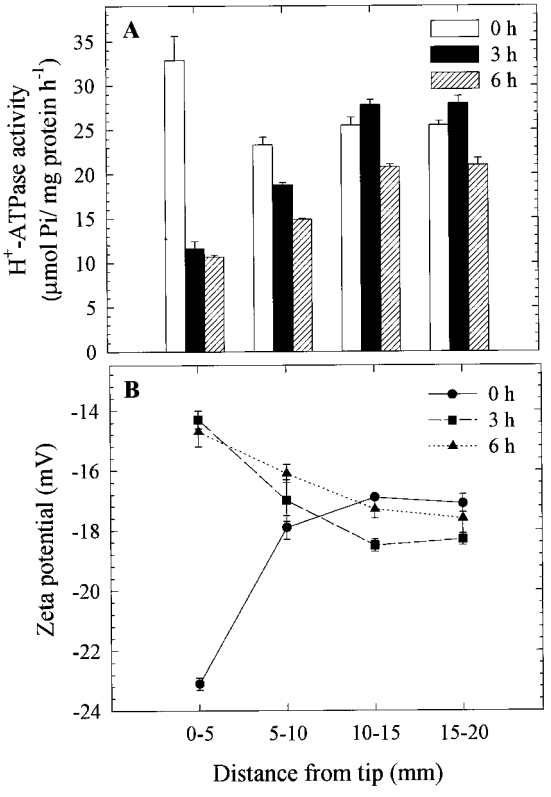

Figure 5. Effect of Al (50 μM) treatment duration in vivo (0, 3, and 6 h) on the H^+-ATPase activity (A) and zeta potential (B) of PM vesicles isolated from specific 5-mm root segment fractions of squash. The plants were grown in HS (one-fifth) adjusted to pH 4.5 for 5 d from germination. Al treatments were performed in the same solution without P, and the plants were cultured in −P solution for at least 12 h prior to treatments. The 5-mm DFT segments were made out of approximately 600 individual plants, and the isolated PM vesicles were pooled to increase the precision of measurement. Values are mean ± SE of three replicates and representative of two independent experiments.

30% higher than in other segments (5–10, 10–15, and 15–20 mm) in the control root, suggesting a developmental control of H^+-ATPase activity along the root apex. It is intriguing that H^+-ATPase activity of PM vesicles isolated from 0- to 5-mm root segments treated with Al in vivo decreased by 64% and 67% after 3- and 6-h treatments, respectively (Fig. 5A). These results suggest that root apex (0–5 mm) is more sensitive to Al in terms of zeta potential and H^+-ATPase activity.

Furthermore, the greater negativity and higher Al binding capacity of the PM vesicles prepared from 0- to 5-mm region of roots were confirmed by the visual evaluation of associated Al with the PM using the fluorescent Al indicator, Morin. Al bound to PM vesicles was determined after Al treatment for 3 and 6 h in vivo (Fig. 6). Al binding to control PM vesicles in vitro was noticeably higher, but it decreased appreciably with vesicles prepared from the roots treated with 50 μM in vivo, (Fig. 6, A and B, bottom). This suggests that the Al bound to PM with in vivo treatment could not be removed after the preparation of vesicles, and this tight binding might cause irreversible alteration to PM properties, which were observed in decreasing Al-binding capacity in vitro (Fig. 6) and increasing zeta potential (Fig. 5).

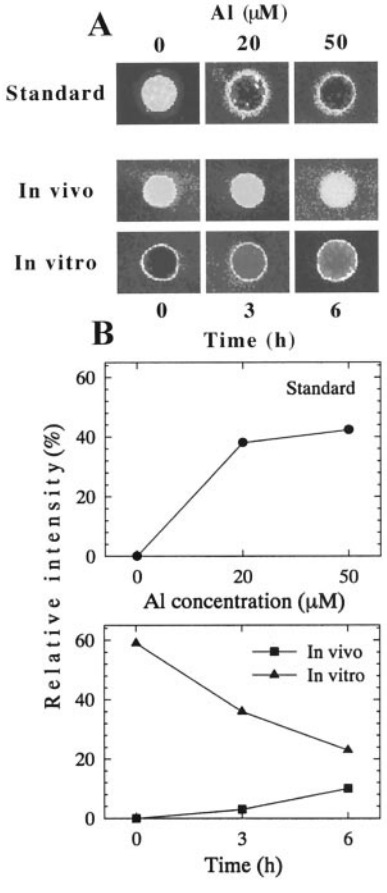

Figure 6. Visualization of Al-induced alteration to the PM property and Al binding capacity of the isolated PM vesicles from squash root apex (0–5 mm) using the Morin assay. A, Calibration (standard) showing a range of Al concentration and the Al-induced fluorescence of control PM vesicles (top); after 50 μM Al treatment in vivo (middle); further addition of 50 μM in vitro (10 min) to the same PM vesicles (bottom). B, Quantitative evaluation of the Morin fluorescence based on the pixel intensity corresponding to images presented in A. Results of standard (top) and after in vivo and in vitro treatments (bottom). For details, see "Materials and Methods."

Impact of Al on the Localization of PM H^+-ATPase in Root Apex

Immunoblot with anti-maize PM H^+-ATPase antibody detected a single band at approximately 100 kD in PM vesicle proteins isolated from 10-mm root apex, showing a high specificity of this antibody to squash PM H^+-ATPase (Fig. 7B). The polyclonal antibody decorated the PM of whole cells along the root apex of controls. However, apical zone cells (0–5 mm) had apparently higher fluorescence compared with the basal zone cells. This was evident from the Figure 7 (set D), demonstrating epidermal (D) and cortex cells (D′) at the 2- to 3-mm region showing bright fluorescence compared with the 7- to 8-mm region of the same root apex (D″). The fluorescence intensity of epidermal cells in the 2- to 3-mm region decreased after 3 h of Al treatment, as did that of the cortex cells (E and E′). However, no obvious differences were perceptible in the 7- to 8-mm mature zone (E″). In contrast, after 6 h of Al treatment, the apex sustained remarkable alteration in the fluorescence, as there was nearly no fluorescence observed on PM from the epidermal (F) and cortex cells (F′). In the case of the 7- to 8-mm region, cells were ripped apart due to Al treatment, and there was no antibody labeling (F″). In addition to these alterations, it is visibly evident from the images that the cells were increasingly swollen with increased duration of Al treatment (3 h, E and E′; 6 h, F and F′) compared with controls (D and D′).

DISCUSSION

Spatial Aspects of Al-Induced Growth Inhibition

The results of our spatial analysis of root growth suggest that the 2- to 4-mm region is the central elongation zone (CEZ) for squash. Al (50 μM) inhibits growth preferentially in this region from 3 h onwards but significantly after 6 h (Fig. 1). The pattern of Al inhibition was similar to the inhibitory effect of Al on maize roots (Blancaflor et al., 1998). The inhibition of total root elongation was derived from the effect on the CEZ. In accordance with our results, Al-induced root growth inhibition occurs only in the few most apical millimeters of the root in maize plants (Ryan et al., 1993; Sivaguru and Horst, 1998). Le Van et al. (1994) described an early (1-h) inhibition of squash root growth by Al, however, those data should be interpreted with caution because of high Al concentrations (1 mM) used. Consistent with the root growth inhibition, higher levels of Al accumulation were also

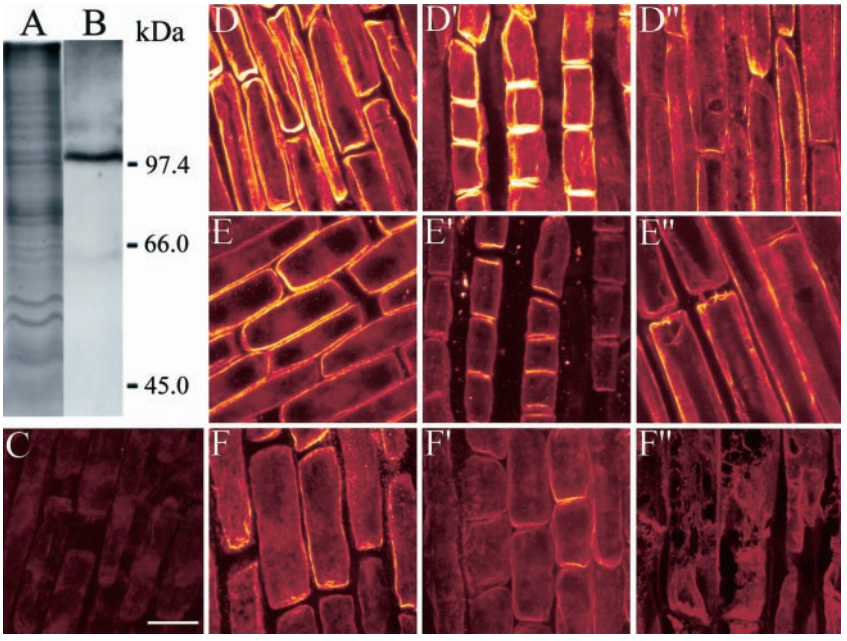

Figure 7. Analysis of the specificity of H^+-ATPase antibody against the isolated PM proteins from squash root apex (10 mm). CB staining (A) and western blot (B). Localization of H^+-ATPase in intact squash root apices (C–F″). Confocal images (for details, see text) of negative control of roots incubated without primary antibody (C). The plants were labeled with the antibody after 0- (D–D″), 3- (E–E″), and 6-h (F–F″) Al (50 μM) treatments. The images are from the 2- to 3-mm DFT of epidermal cells (D–F), cortex (D′, E′, and F″) and 7- to 8-mm DFT of epidermal cells (D″, E″, and F″). Note the decrease in the intensity of H^+-ATPase upon time after Al treatments compared with control counterparts along the root apex. Bar = 40 μm.

found at the 2- to 4-mm CEZ region (Fig. 2). An increased Al accumulation at narrow zones (2-mm segments) of wheat (Rincon and Gonzales, 1992; Tice et al., 1992; Samuels et al., 1997) and 1-mm segments of maize (Sivaguru and Horst, 1998) showed similar patterns of growth inhibition to those observed in squash.

Impact of Al on PM Properties and Its Association with H^+-ATPase

Intact seedlings have an undiminished or even enhanced capacity for proton secretion in Al solution even after 24 h in 100 μM $AlCl_3$ (Kinraide, 1988). In contrast, vesicles isolated from Al-treated seedlings exhibit a diminished H^+-ATPase activity. There was a weak inhibition (11%) of H^+-ATPase activity of microsomal membranes prepared from whole-root of barley (Matsumoto, 1988; Matsumoto et al., 1992), a 12% inhibition in the Al-tolerant wheat (cv Atlas 66), and 18% in the Al-sensitive wheat (cv Scout 66) after the treatment with 50 μM Al for 1 d (Sasaki et al., 1995). However, we show much higher level of H^+-ATPase inhibition in purified PM preparations isolated from specific 5-mm root apex but not from whole roots (Figs. 3 and 4). Preliminary experiments indicated that a relationship does exist between the less negativity of zeta potential and decreased H^+-ATPase activity of PM vesicles under a range of external pH (data not shown). It is interesting that this relationship was observed in PM vesicles isolated from Al-treated squash roots and was more conspicuous in the PM vesicles isolated from root apex 5 mm from root tip, which was the most sensitive region to Al toxicity (Figs. 3 and 4). The mechanism underlying this event might be related to the inhibition of H^+-efflux through PM by H^+-pumping due to the depolarization of surface potential under Al stress. The question arises whether this kind of event is true for other cations. Another alteration of membrane property induced by metal binding could be a reduction in the accessibility of toxic cations due to altered surface electrical change.

With intense research on the relationship between Al and PM electrical properties, several reports proposed that the PM depolarization is itself may be an inhibitory stress (see introduction). This would be in agreement with the observation that all polycationic (charge $\geq$3+) ions are toxic and that small ions are more toxic than larger ones ($Al^{3+} > La^{3+} > TEC^{3+}$) in accordance with the capacity for depolarization. The enhanced toxicity of H^+ could be rationalized in this way relative to the toxicity of Na^+ and K^+. However, all of these toxicities can be relieved by treatments that reduce surface negativity. In accordance with this idea, alleviation of Al toxicity is achieved by treatments that reduce the negativity of cell-surface electrical potential, for instance by the addition of Ca^{2+}, thus restricting the accessibility of Al to membrane (Kinraide et al., 1992, 1998; Kinraide, 1994).

To understand the degree of depolarization of the membrane surface by Al, we compared the depolarization induced by Ca^{2+} (data not shown) and Al in vitro (Fig. 4, A and B). The depolarization of zeta potential by Ca^{2+} in vitro was slight (10%) compared with Al and may not be sufficient to cause the inhibition of H^+-ATPase activity. In other words, the distinct depolarization of PM zeta potential by Al may cause the inhibition of H^+-ATPase activity (Fig. 5). These observations suggest that more negativity of a resting potential combined with a higher depolarization of surface potential may be associated with

sensitivity to Al toxicity. Nevertheless, whether these events are triggered by a trans-membrane potential difference (E_m) needs be determined by measuring the E_m from the intact roots.

The determination of zeta potential (Fig. 4) and Al binding with membrane using the Morin assay (Fig. 6) after in vitro Al treatment revealed intriguing results. These results suggest that (a) in vivo Al treatment caused depolarization of surface potential, which could not be further depolarized by the externally added Al in vitro (Fig. 4C), (b) this was understandable because Al was remained in membrane vesicles after isolation (Fig. 6), and (c) both phenomena were confirmed by much less binding of externally added Al to PM vesicles isolated from Al-treated roots in vivo compared with higher Al binding to the control PM vesicles (Fig. 6). Taken together, these experiments provide insights into the tight Al binding to PM in the 0- to 5-mm region of the root apex and altered membrane property by in vivo Al treatments.

Further, immunofluorescence studies using maize PM H^+-ATPase antibody coupled with confocal laser scanning microscopy confirmed the above results as we found abundant H^+-ATPase localized in 2- to 3-mm epidermal and cortex cells compared with mature zones at 7 to 8 mm (Fig. 9, set D). The outcome of this experiment supports the prevailing hypothesis that high levels of H^+-ATPase are present in cells engaged in active transport (Serrano, 1985). The images are comparable with the highly abundant, asymmetrically localized H^+-ATPase in cells closer to the root-soil interface, i.e. epidermal and outer cortex tissues in maize root apices (Jahn et al., 1998). In accordance with the measured decline in H^+-ATPase activity, there was a steady decline in the H^+-ATPase fluorescence at 2- to 3-mm region following Al treatments as compared with all other regions (Fig. 7). This may be due to an Al-induced decrease in the H^+-ATPase protein per unit area of the PM (Yan et al., 1998) or alteration to stoichiometric configuration of the auto-inhibitory domain in the C terminus of H^+-ATPase (Sze et al., 1999) concomitant with inhibition of enzyme activity by direct interaction with Al, limiting the antibody cross reactivity with H^+-ATPase.

Although reports supporting extracellular target sites for Al toxicity are abundant, studies implying direct Al interaction with cytoplasmic target sites are few. However, several reports do confirm the cytoplasmic target sites of Al, such as direct Al binding to the nuclei (Matsumoto et al., 1976; Silva et al., 2000), which are enabled by Al penetration through the PM (Taylor et al., 2000). Our report may provide circumstantial evidence in this line as H^+-ATPase is localized in the cytoplasmic domain, and direct Al binding and interaction with this protein complex is not ruled out.

MATERIALS AND METHODS

Growth Conditions and Root Growth Measurements

Squash (*Cucurbita pepo* L. cv Tetsukabuto) seeds were soaked in tap water for 12 h and germinated in an incubator (28°C) in the dark for 24 h on two layers of filter paper saturated with 1/5 Hoagland solution (HS) adjusted to pH 4.5 with 0.1 M HCl. After germination, uniform seedlings with 1.5-cm root length were transferred to polyethylene pots and grown in a controlled-environment chamber with a 14-h-day/10-h-night cycle under 580 μmol m^{-2} s^{-1} of light during the day. The day night temperatures were set at 25°C/20°C with 65% constant relative humidity. The HS was continuously aerated and replaced everyday to maintain constant pH.

Five-day-old seedlings were transferred to a modified HS without phosphate at least 12 h prior to root growth experiments. The segmental (2-mm) elongation rate was measured after marking the 2-mm positions up to 10 mm of the apex using a fine brush with Indian ink. The plants with marked roots were transferred to HS containing 0 or 50 μM Al (pH 4.5) without phosphate, and the movement of markings on growing roots was photographed at designated times using a stereo microscope (Zeiss-Stemi 2000-C, Carl-Zeiss, Oberkochen, Germany equipped with a CCD-color video camera, Sony, Tokyo). The exact segmental elongation was determined later from the digitized images saved in the computer using Mac Scope (version 2.56) software.

Quantification of Al in Root Segments

After designated Al treatments (0, 3, and 6 h), the roots were washed in double-distilled water and cut into five consecutive 2-mm segments starting from the apex including the root cap using a razor blade. The excised individual 2-mm segments or 10-mm whole root apices (four replicate segments) were transferred to 1.5-mL Eppendorf (Netheler-Hinz Gmbh, Hamburg, Germany) cups each containing 1 mL of 2 M HCl for 48 h. The Al-contents in HCl solution were determined by an atomic absorption spectrophotometer (Z-8270, Hitachi, Tokyo) after dilution.

Preparation of PM Vesicles

PM vesicles were prepared strictly at 4°C following the method of Palmgren et al. (1990). Briefly, after Al treatments, the whole-root (5 g fresh weight) and the root segments from primary roots of approximately 600 plants (constituting approximately 1 g fresh weight) were ground in the presence of insoluble polyvinylpyrrolidone with a homogenizing buffer having 330 mM Suc, 50 mM MOPS-1,3-bis(Tris[hydroxymethyl]methylamino) propane (BTP), pH 7.0, 5 mM EDTA, 5 mM dithiothreitol (DTT), 0.5 mM phenylmethylsulfonyl fluoride, 0.2% (w/v) bovine serum albumin (Sigma, Tokyo, protease free), and 0.2% (w/v) casein. The homogenate was filtered through four layers of cheesecloth and centrifuged (10,000*g*, 20 min). The supernatant was ultra-centrifuged (100,000*g*, 1 h), and the result-

ing precipitate was resuspended with a glass homogenizer in suspension buffer consisting of 330 mM Suc, 5 mM K-phosphate (pH 7.5), 5 mM KCl, 1 mM DTT, and 0.1 mM EDTA. The homogenate was loaded on a 12-g two-phase system containing 6.5% (w/w) Dextran T500, 6.5% (w/w) polyethylene glycol 3350, 330 mM Suc, 5 mM K-phosphate (pH 7.8), 5 mM KCl, 1 mM DTT, and 0.1 mM EDTA. After the batch procedure, the resulting upper phase was mixed with a dilution buffer that consisted of 330 mM Suc, 5 mM MOPS-BTP (pH 7.5), and 5 mM KCl and centrifuged (100,000*g*, 1h). For the determination of zeta potential, the PM vesicles were used immediately, or stored otherwise at −80°C until further analysis.

Determination of H^+-ATPase Activity in PM Vesicles

H^+-ATPase activity was measured in an assay system containing 50 mM MOPS-BTP (pH 6.5), 2.5 mM $MgSO_4$, 50 mM KCl, 2.5 mM Tris-ATP, 0.05% (w/w) Brij 58 (polyoxyethylene 20 cetyl ether, Sigma, Tokyo) to produce inside-out vesicles (Johansson et al., 1995) and an appropriate amount of H^+-ATPase. The reaction was carried out for 30 min at 37°C. Five-hundred microliters of 5% (w/v) cold trichloroacetic acid and 2 mL of 0.1 M Na-acetate was added to the mixture and centrifuged (2,000*g*, 10 min) with a further addition of 0.3 mL of 1% (w/v) ammonium molybdate in 0.025 M H_2SO_4. After a brief incubation (30°C, 10 min), the liberated Pi was measured with a spectrophotometer (model UV-1201; Shimadzu, Japan) at 720 nm. The membrane protein was determined with the Bradford (1976) method using bovine serum albumin as standard.

Determination of Zeta Potential in PM Vesicles Using Light Scattering Electrophoresis

Zeta potential was determined using the ELS-8000 apparatus (OTSUKA Electronics LTD, Japan). Zeta potential (which approximates the surface potential) of PM vesicles isolated from whole-root and 5-mm root segments from the tip (control and after Al treatments) was calculated from the electrophoretic mobility determined by means of free-flow electrophoresis. All other parameters were followed as described previously (Gimmler et al., 1991). The electrophoresis medium (chamber buffer) contained 330 mM Suc, 5 mM MOPS-1,3-bis(Tris[hydroxymethyl]methylamino) propane (pH 7.5), 5 mM KCl. This buffer was presterilized by passing through a glass fiber filter followed by a 0.45-μm membrane filter. Cells were washed several times in chamber buffer and kept for at least 30 min prior to measurement. Freshly isolated right-side-out PM vesicles (10-μg PM protein equivalent) were diluted 100 times with the same buffer and kept at 25°C for 10 min in the presence or absence of various levels of Al or Ca. The sample was then added in an acrylic electrophoresis cell, and measurements were performed in a computer connected with the detection system. After each measurement, cells were washed several times in chamber buffer, and the measurement proceeded. In the case of in vitro measurements, the dissociation of ions from the cell surface during the electrophoretic run was avoided by maintaining the appropriate concentrations of Al or Ca in the chamber buffer. The zeta potential was determined using Latex (Dow Chemical, Tokyo) as a standard. The computer-aided measurement of zeta potential (ζ) of PM vesicles was calculated from the electrophoretic mobility (μ) using the Smoluchowski equation:

$$\zeta = \mu\eta/\varepsilon\varepsilon_o$$

where η is the viscosity, ϵ is the relative dielectric constants of the buffer, and ε_o is the dielectric constant of vacuum (Gimmler et al., 1991).

Assay of Al Binding Property of PM Vesicles

We developed a new method to visually evaluate the Al binding to PM vesicles and at the same time to assess the alteration of the PM property induced by Al. The PM vesicles from 0- to 5-mm root segments after 0, 3, and 6 h of Al (50 μM) treatments were used for this purpose. The 0-h PM vesicles (10-μg PM protein basis) were used for a calibration as they have been incubated in solutions containing 0, 20, or 50 μM Al (final concentration) for 10 min in vitro. The PM vesicles isolated after 3 and 6 h of Al treatment in vivo were further incubated (10-μg PM protein basis) with either 0 or 50 μM Al for 10 min in vitro. After incubations, the PM vesicles were blotted carefully as a spot onto a polyvinylidene difluoride membrane (2 × 2 cm) under vacuum. After a brief wash, the membranes were completely dried and transferred to 10 mM MES buffer (pH 5.5) containing 100 μM Morin (15 min). The stained membranes were dried after a brief wash and scanned directly at appropriate excitation and emission wavelengths (as described previously) of Morin using an Intelligent Dark Box II (Fuji film, LAS-1000, Tokyo), and the pixel intensities were quantified using the Image Gauge (version 3.3) software.

Immunolocalization of PM H^+-ATPase Using Confocal Laser Scanning Microscopy

The electrophoresed (Laemmli, 1970) PM proteins were electroblotted onto polyvinylidene difluoride membrane, and the H^+-ATPase was detected using standard western-blot protocol with an antibody raised against maize H^+-ATPase.

Immunolocalization of H^+-ATPase was performed essentially as described in Sivaguru et al. (1999). Briefly, after designated treatments, the root apices (10 mm) were dissected and transferred to 5 mL of stabilizing buffer (SB: 50 mM PIPES, 5 mM EGTA, and 5 mM $MgSO_4$, pH 6.9) containing 5% (v/v) dimethyl sulfoxide for 15 min at room temperature. They were then fixed with 4% (w/v) paraformaldehyde in SB containing 10% (v/v) dimethyl sulfoxide for 60 min at room temperature with initial 10 min under vacuum. After three 10-min rinses in PBS (pH 7.4), to facilitate antibody penetration, they were digested with an enzymatic cocktail (1% [w/v] Hemicellulase [from *Aspergillus niger*, Sigma-Aldrich, Tokyo], 1% [w/v] Pectolyase

[Seishin Corporation, Tokyo], 0.5 M EGTA, 0.4 M Mannitol, 1% [v/v]Triton X-100, 0.3 mM phenylmethylsulfonyl fluoride, all dissolved in SB) for 60 min. The digestion reaction was terminated by transferring the roots to SB for 15 min followed by 1% (v/v) Triton X-100 in SB for 10 min. After a brief rinse in SB, the samples were extracted in HPLC grade absolute methanol at −20°C, rehydrated in PBS (2 h), and incubated with rabbit polyclonal antibody raised against maize H^+-ATPase diluted 1:200 in PBS for 12 h in dark at room temperature. The roots were then incubated with TRITC conjugated anti-rabbit IgG raised in goat (Sigma-Aldrich, Tokyo) diluted 1:100 in PBS for 12 h at room temperature. Parallel sets of roots processed without primary antibodies served as negative controls. The procedure was completed by transferring the labeled roots to 0.01% (w/v) Toluidine Blue in PBS to diminish the autofluorescence of the tissue and mounted in Mowiol (Calbiochem, La Jolla, CA).

The images of H^+-ATPase from roots were obtained using the 543-nm excitation line of He-Ne laser fitted in a Zeiss confocal microscope (see above) using Ph3-Plan-Neofluar 100× oil immersion objective. The root surface images were the overlay of 7 to 11 optical sections (0.75 μm thick), and scan configurations were kept constant between treatments using the recycle option of the LSM 510 software to assess the intensity differences among treatments. The images were organized using Adobe Photoshop 4.0J (Adobe Systems, San Jose, CA) and printed using Fujix-3000 Pictography digital printer (Fuji-Film, Tokyo).

ACKNOWLEDGMENTS

We thank Prof. Hideo Sasagawa, Okayama University for kindly supplying H^+-ATPase primary antibody, and we are indebted to Dr. Michael Keller, Division of Biological Sciences, University of Missouri, Columbia, MO, for critical reading and corrections on the text.

Received December 1, 2000; returned for revision February 11, 2001; accepted April 24, 2001.

LITERATURE CITED

Ahn SJ, Im YJ, Chung GC, Cho BH (1999) Inducible expression of plasma membrane H^+-ATPase in the roots of figleaf gourd plants under chilling root temperature. Physiol Plant **106:** 35–40

Blancaflor EB, Jones D, Gilroy S (1998) Alterations in the cytoskeleton accompany aluminum-induced growth inhibition and morphological changes in primary roots of maize. Plant Physiol **118:** 159–172

Bradford MM (1976) A rapid and sensitive method for the quantitation of microgram quantities of protein utilizing the principle of protein-dye binding. Anal Biochem **72:** 248–254

Gimmler H, Treffny B, Kowalski M, Zimmermann U (1991) The resistance of *Dunaliella acidophila* against heavy metals: the importance of the zeta potential. J Plant Physiol **138:** 708–716

Horst WJ (1995) The role of the apoplast in aluminum toxicity and resistance of higher plants: a review. Z Pflanzenernäehr Bodenkd **158:** 419–428

Jahn T, Baluska F, Michalke W, Harper JF, Volkmann D (1998) Plasma membrane H^+-ATPase in the root apex: evidence for strong expression in xylem parenchyma and asymmetric localization within cortical and epidermal cells. Physiol Plant **104:** 311–316

Johansson F, Olbe M, Sommarin M, Larsson C (1995) Brij 58, a polyoxyethylene acyl ether, creates membrane vesicles of uniform sideness: a new tool to obtain inside-out (cytoplasmic side-out) plasma membrane vesicles. Plant J **7:** 165–173

Jones DL, Kochian LV (1997) Aluminum interaction with plasma membrane lipids and enzyme metal binding sites and its potential role in Al cytotoxicity. FEBS Lett **400:** 51–57

Kinraide TB (1988) Proton extrusion by wheat roots exhibiting severe aluminum toxicity symptoms. Plant Physiol **88:** 418–423

Kinraide TB (1994) Use of a Gouy-Chapman-Stern model for membrane-surface electric potential to interpret some features of mineral rhizotoxicity. Plant Physiol **106:** 1583–1592

Kinraide TB, Ryan PR, Kochian LV (1992) Interactive effects of Al^{3+}, H^+, and other cations on root elongation considered in terms of cell-surface electrical potential. Plant Physiol **99:** 1461–1468

Kinraide TB, Yermiyahu U, Rytwo G (1998) Computation of surface electrical potentials of plant cell membranes: correspondence to published zeta potentials from diverse plant sources. Plant Physiol **118:** 505–512

Kochian LV (1995) Cellular mechanisms of aluminum toxicity and resistance in plants. Annu Rev Plant Physiol Plant Mol Biol **46:** 237–260

Laemmli UK (1970) Cleavage of structural proteins during the assembly of the head of bacteriophage T4. Nature **227:** 680–685

Le Van H, Kuraishi S, Sakurai N (1994) Aluminum-induced rapid root inhibition and changes in cell-wall components of squash seedlings. Plant Physiol **106:** 971–976

Matsumoto H (1988) Inhibition of proton transport activity of microsomal membrane vesicles of barley roots by aluminum. Soil Sci Plant Nutr **34:** 499–506

Matsumoto H (2000) Cell biology of Al tolerance and toxicity in higher plants. Int Rev Cytol **200:** 1–46

Matsumoto H, Hirasawa E, Torikai H, Takahoshi E (1976) Localization of absorbed aluminum in pea root and its binding to nucleic acids. Plant Cell Physiol **17:** 127–137

Matsumoto H, Yamamoto Y, Kasai M (1992) Changes of some properties of the plasma membrane-enriched fraction of barley roots related to aluminum stress: membrane-associated ATPase, aluminum and calcium. Soil Sci Plant Nutr **38:** 411–419

Miyasaka SC, Kochian LV, Shaff JE, Foy CD (1989) Mechanism of aluminum tolerance in wheat: an investigation of genotypic differences in rhizosphere pH, K^+, and H^+ transport, and root-cell membrane potentials. Plant Physiol **91:** 1188–1196

Palmgren MG, Askerlund P, Fredrikson K, Widell S, Sommarin M, Larsson C (1990) Sealed inside-out and right-side-out plasma membrane vesicles: optimal conditions for formation and separation. Plant Physiol **92:** 871–880

Rengel Z (1996) Uptake of aluminum by plant cells. New Phytol **143:** 389–406

Rincon M, Gonzales RA (1992) Aluminum partitioning in intact roots of aluminum-tolerant and aluminum-sensitive wheat (*Triticum asetivum* L.) cultivars. Plant Physiol **99:** 1021–1028

Ryan PR, DiTomaso JM, Kochian LV (1993) Aluminum toxicity in roots: an investigation of spatial sensitivity and the role of the root cap. J Exp Bot **44:** 437–446

Samuels TD, Kücükakyüz K, Rincon M (1997) Al partitioning patterns and root growth as related to Al sensitivity and Al tolerance in wheat. Plant Physiol **113:** 527–534

Sasaki M, Kasai M, Yamamoto Y, Matsumoto H (1995) Involvement of plasma membrane potential in the tolerance mechanism of plant roots to aluminum toxicity. *In* RA Date, NJ Grundon, GF Rayment, MF Probert, ME, eds, Plant-Soil Interactions at Low pH. Kluwer Academic Publishers, Dordrecht, The Netherlands, pp 285–290

Serrano R (1985) Plasma membrane ATPase of plants and fungi. CRC Press, Boca Raton, FL

Siegel N, Haug A (1983) Calmodulin-dependent formation of membrane potential in barley root plasma membrane vesicles: a biochemical model of aluminum toxicity in plants. Physiol Plant **59:** 285–291

Silva IR, Smyth J, Moxley DF, Carter TE, Allen NS, Rufty TW (2000) **A**luminum accumulation at nuclei of cells in the root tip: fluorescence detection using lumogallion and confocal laser scanning microscopy. Plant Physiol **123:** 543–552

Sivaguru M, Baluška F, Volkmann D, Felle HH, Horst WJ (1999) Impacts of aluminum on the cytoskeleton of the maize root apex: short-term effects on the distal part of the transition zone. Plant Physiol **119:** 1073–1082

Sivaguru M, Horst WJ (1998) The distal part of the transition zones is the most aluminum-sensitive apical root zone of maize. Plant Physiol **116:** 155–163

Suhayda CG, Giannini JL, Briskin DP, Shannon MC (1990) Electrostatic changes in *Lycopersicon esculentum* root plasma membrane resulting from salt stress. Plant Physiol **93:** 471–478

Sussman MR (1994) Molecular analysis of proteins in the plant plasma membrane. Annu Rev Plant Physiol Plant Mol Biol **45:** 211–234

Sze H, Li X, Palmgern MG (1999) Energization of plant cell membranes by H^+-pumping ATPases: regulation and biosynthesis. Plant Cell **11:** 677–689

Taylor GJ (1995) Overcoming barriers to understanding the cellular basis of aluminum resistance. Plant Soil **171:** 89–103

Taylor GJ, McDonald-Stephens JL, Hunter DB, Bertsch PM, Elmore D, Rengel Z, Reid RJ (2000) Direct measurement of aluminum uptake and distribution in single cells of *Chara corallina*. Plant Physiol **123:** 987–996

Tice KR, Parker DR, DeMason DA (1992) Operationally defined apoplastic and symplastic aluminum fractions in root tips of aluminum-intoxicated wheat. Plant Physiol **100:** 309–318

Vose PB, Randall PJ (1962) Resistance to aluminum and manganese toxicities in plants related to variety and cation-exchange capacity. Nature **196:** 85–86

Wagatsuma T, Akiba R (1989) Low surface negativity of root protoplasts from aluminum-tolerant plant species. Soil Sci Plant Nutr **35:** 443–452

Yan F, Feuerle R, Schäffer S, Fortmeier H, Schubert S (1998) Adaptation of active proton pumping and plasmalemma ATPase activity of corn roots to low root medium pH. Plant Physiol **117:** 311–319

Yermiyahu U, Brauer DK, Kinraide TB (1997) Sorption of aluminum to plasma membrane vesicles isolated from roots of Scout 66 and Atlas 66 cultivars of wheat. Plant Physiol **115:** 1119–1125

Young JC, DeWitt ND, Sussman MRA (1998) A transgene encoding a plasma membrane H^+-ATPase that confers acid resistance in *Arabidopsis thaliana* seedlings. Genetics **149:** 501–507